

On the Spectroscopy of Phosphaalkynes: Millimeter- and Submillimeter-Wave Study of C_2H_5CP

Luis Bonah,[†] Stephan Schlemmer,[†] Jean-Claude Guillemin,[‡] Michael E.
Harding,[¶] and Sven Thorwirth^{*,†}

[†]*I. Physikalisches Institut, Universität zu Köln, Zùlpicher Str. 77, 50937 Köln, Germany*

[‡]*Univ Rennes, Ecole Nationale Supérieure de Chimie de Rennes, CNRS, ISCR –
UMR6226, 35000 Rennes, France*

[¶]*Institut für Nanotechnologie, Karlsruher Institut für Technologie (KIT), Kaiserstr. 12,
76131 Karlsruhe, Germany*

E-mail: sthorwirth@ph1.uni-koeln.de

Abstract

Ethyl phosphoethyne, C_2H_5CP , has been characterized spectroscopically in the gas phase for the first time, employing millimeter- and submillimeter-wave spectroscopy in the frequency regime from 75 to 760 GHz. Spectroscopic detection and analysis was guided by high-level quantum-chemical calculations of molecular structures and force fields performed at the coupled-cluster singles and doubles level extended by a perturbative correction for the contribution from triple excitations, CCSD(T), in combination with large basis sets. Besides the parent isotopologue, the three singly substituted ^{13}C species were observed in natural abundance up to frequencies as high as 500 GHz. Despite the comparably low astronomical abundance of phosphorus, phosphoalkynes, R-CP, such as C_2H_5CP are promising candidates for future radio astronomical detection.

Introduction

Nitriles, chemical species of the general formula R-CN, are one if not the most prominent class of molecules found in space. Over the last fifty

years, many nitriles have been detected by their pure rotational spectra using radio astronomical techniques. Here, species range from simple prototypical HCN,¹ over metal-bearing variants like FeCN² and CN-bearing molecular ions^{3,4} up to complex and heavy benzenoid variants such as cyanonaphthalene⁵ and cyanoindene,⁶ just to name a few.

Owing to intrinsically strong dipole moments, numerous nitriles have also been studied in the laboratory using microwave and millimeter-wave spectroscopy. In contrast, comparable studies of phosphoalkynes, where the CN functional group is replaced by an isovalent CP unit, are rather scarce, which may in part be attributed to their pronounced transient character and also more challenging synthetic routes. Since the first microwave spectroscopic studies of prototypical phosphoethyne (HCP),⁷ and a handful of other selected species studied by Kroto and collaborators (HC₃P, CH₃CP, NCCP, C₂H₃CP, PhCP; see Burckett-St. Laurent et al.⁸ and references therein), only a small number of additional phosphoalkynes have been characterized employing high-resolution (rotational) spectroscopy. For detailed accounts on the available laboratory spectroscopic data of individual species, the inter-

ested reader may consult the reports on phosphoethyne, HCP,^{9,10} HC₃P,^{9,11} HC₅P,^{12,13} NCCP,⁹ NC₄P,^{14,15} C₂H₃CP,¹⁶ CH₃CP,^{17,18} PhCP,¹⁹ and C₃H₅CH₂CP.²⁰

It should be noted that while to this day spectroscopic signatures of only two phosphoalkynes, HCP and NCCP, have been found in space^{21,22} not all of the above species have yet been characterized in the laboratory at a level meeting the needs of radio astronomy. In addition, other potentially astronomically relevant phosphoalkynes still await laboratory (high-resolution) spectroscopic characterization. One such species is ethyl phosphoethyne, C₂H₅CP (also known as propylidynephosphine or phosphabutyne).

C₂H₅CP, the phosphorus variant of the astronomically ubiquitous ethyl cyanide, C₂H₅CN (e.g. Endres et al.²³), has been known in the laboratory for many years and characterized by its ¹H, ³¹P, and ¹³C NMR spectra in solution.^{24,25} However, so far, there does not seem to be any account of its spectroscopic properties in the gas phase. In the present study, high-level quantum-chemical calculations were performed at the coupled-cluster (CC) singles and doubles level extended by a perturbative correction for the contribution from triple excitations, CCSD(T). Based on these results, the pure rotational spectrum of C₂H₅CP has been detected for the first time and observed in selected frequency ranges between 75 and 760 GHz. A detailed account of the experimental and theoretical work as well as the analysis of the rotational spectrum of C₂H₅CP in its ground vibrational state will be given in the following.

Theoretical and Experimental Methods

Quantum-Chemical Calculations

Quantum-chemical calculations to guide the spectroscopic search of C₂H₅CP were performed at the CC singles and doubles level extended by a perturbative correction for the contribution from triple excitations (CCSD(T)).²⁶ All calculations were performed using the quantum-

chemical program package CFOUR.^{27–29} Correlation-consistent polarized valence and polarized core valence basis sets were used throughout. Within the frozen core (fc) approximation, the tight-*d*-augmented basis set cc-pV(T+*d*)Z was used for the phosphorus atom, and the corresponding cc-pVTZ basis sets for carbon and hydrogen^{30,31} as well as the atomic natural orbital basis set ANO1.³² The ANO1 set consists of 18s13p6d4f2g to 5s4p2d1f, 13s8p6d4f2g to 4s3p2d1f, and 8s6p4d3f to 4s2p1d contractions for P, C, and H, respectively.

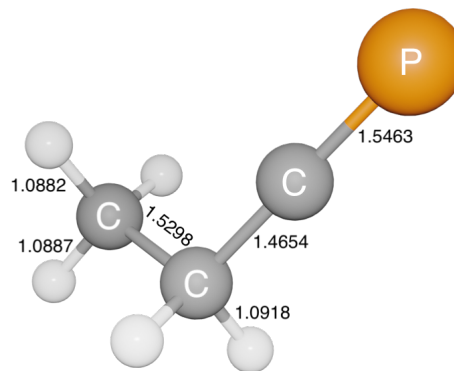


Figure 1: Bond lengths of C₂H₅CP calculated at the ae-CCSD(T)/cc-pwCVQZ level of theory (in Å). Full structure in internal coordinates is given in the Supporting Information.

The cc-pwCVXZ (X = T and Q) basis sets were used when considering all electrons in the correlation treatment.³³ Equilibrium geometries were obtained using analytic gradient techniques.³⁴ For molecules comprising first and second-row elements, the ae-CCSD(T)/cc-pwCVQZ level of theory has been shown on many occasions to yield molecular equilibrium structures of very high quality (e.g., Coriani et al.³⁵). The corresponding structure of C₂H₅CP is shown in Figure 1. Full sets of internal coordinates of both the ground state molecular structure and the transition state to methyl internal rotation are collected in the Supporting Information.

Harmonic and anharmonic force fields were calculated in the fc approximation using the cc-pV(T+*d*)Z and ANO1 basis sets using analytic second-derivative techniques,^{36,37} followed by additional numerical differentiation to calculate

the third and fourth derivatives needed for the anharmonic force field.^{37,38} Theoretical ground-state rotational constants were then estimated from the equilibrium rotational constants (calculated at the CCSD(T)/cc-pwCVQZ level of theory) and the zero-point vibrational corrections ΔA_0 , ΔB_0 , and ΔC_0 (calculated at the fc-CCSD(T)/ANO1 level, see Table 1). In addition, the fc-CCSD(T)/ANO1 force field calculation yields the quartic and sextic centrifugal distortion parameters. Spin-rotation constants, owing to the presence of ^{31}P ($I = 1/2$), were calculated at the CCSD(T)/cc-pwCVQZ level of theory using rotational London orbitals.³⁹

At the ae-CCSD(T)/cc-pwCVQZ level of theory and corrected for harmonic zero-point effects at the fc-CCSD(T)/ANO1 level of theory, the barriers of internal rotation V_3 of both $\text{C}_2\text{H}_5\text{CP}$ and isovalent $\text{C}_2\text{H}_5\text{CN}$ are estimated as about 2.8 kcal/mol, suggesting that torsional splitting will not be significant for the ground state rotational spectrum obtained here.

Puzzarini et al.⁴⁰ may be consulted for further insight into the theoretical approaches used in the present context.

Experiment

Broadband measurements were recorded with a synthesized sample using three different experimental setups in Cologne. The three measured frequency ranges of 75–120 GHz, 170–255 GHz, and 340–760 GHz resulted in a total frequency coverage of 550 GHz.

Synthesis

$\text{C}_2\text{H}_5\text{CP}$ was prepared following the synthesis published by Guillemin et al.²⁵. The three-step sequence involves the synthesis of 1,1-dichloropropylphosphonic acid diisopropyl ester which was reduced to 1,1-dichloropropylphosphine, followed by a bis-dehydrochlorination using 1,8-diazabicyclo[5.4.0]undec-7-ene as a base to generate $\text{C}_2\text{H}_5\text{CP}$. The two last steps of the synthesis were performed in tetraethylene glycol dimethyl ether (tetraglyme) as solvent. $\text{C}_2\text{H}_5\text{CP}$ was purified by vaporization, condensed under vacuum at

–100 °C, and finally introduced into a cell containing degassed tetraglyme for storage at dry ice temperature.

Broadband Measurements

Spectra were obtained through broadband scans by utilizing three different absorption experiments sharing a common basic structure consisting of a source, an absorption cell, and a detector. The sources consist of synthesizers and subsequent commercial amplifier-multiplier chains to reach the desired frequency range. For the absorption cells, different lengths of borosilicate tubes were used. The resulting radiation was propagated via horn antennas, mirrors, and polarization filters through the absorption cells and onto the detectors. These are either Schottky detectors (< 500 GHz) or a cryogenically cooled bolometer (> 500 GHz). All experiments utilized frequency modulation with a $2f$ -demodulation scheme to increase the SNR. The resulting lineshapes look similar to the second derivative of a Voigt profile. More in-depth descriptions of the setups have been given earlier in Martin-Drumel et al.⁴¹, Zingsheim et al.⁴².

All measurements were performed at room temperature and static pressure. This was deemed safe as a time series of the same calibration line showed no significant degradation of the sample over time. Before each filling of the absorption cells, the sample was frozen out. Then, $\text{C}_2\text{H}_5\text{CP}$ was selectively removed from the solution *in vacuo* while keeping the sample container at a temperature of about –40 °C. The filling pressures were in the range of 10–40 μbar . Reproducibility lines were measured before and after each batch of measurements as sanity checks (see Supporting Information). Standing waves were removed from the broadband spectra via Fourier filtering with an in-house written script¹.

¹Available at <https://github.com/Ltotheo/SnippetsForSpectroscopy/tree/main/FFTCorrection>

Table 1: Calculated and experimental molecular parameters of C_2H_5CP in its ground vibrational state.

Parameter	Calculations	Experimental
A_e / MHz	25 374.531	...
B_e / MHz	2719.663	...
C_e / MHz	2532.995	...
ΔA_0 / MHz	158.770	...
ΔB_0 / MHz	12.603	...
ΔC_0 / MHz	14.132	...
A_0 / MHz	25 215.761	25 216.122 85(35)
B_0 / MHz	2707.060	2709.143 447(22)
C_0 / MHz	2518.863	2520.638 536(21)
$-D_J$ / Hz	-879.142	-900.7695(38)
$-D_{JK}$ / kHz	23.760	24.101 222(85)
$-D_K$ / kHz	-536.855	-547.7691(34)
d_1 / Hz	-147.802	-153.7099(23)
d_2 / Hz	-7.414	-8.116 25(97)
H_J / mHz	1.461	1.504 07(31)
H_{JK} / mHz	-14.470	-14.8371(54)
H_{KJ} / Hz	-1.374	-1.377 47(40)
H_K / Hz	36.623	36.895(11)
h_1 / μ Hz	469.5	490.70(24)
h_2 / μ Hz	65.5	69.37(13)
h_3 / μ Hz	6.8	6.570(15)
L_J / nHz	...	-3.0130(87)
L_{JK} / μ Hz	...	-2.446(11)
L_{KKJ} / μ Hz	...	71.50(53)
l_1 / nHz	...	-1.3244(74)
l_2 / pHz	...	-259.3(50)
$C_{aa}(P)$ / kHz	7.42	...
$C_{bb}(P)$ / kHz	5.02	...
$C_{cc}(P)$ / kHz	4.92	...
$C_{ab}(P)$ / kHz	12.51	...
$C_{ba}(P)$ / kHz	1.06	...
μ_a / D	1.53	...
μ_b / D	0.29	...
V_3 / kcal/mol	2.8	...
Transitions	...	6016
Lines	...	4010
RMS / kHz	...	29.7
$WRMS$...	1.00

Notes. Fits performed with SPFIT in the S -reduction and the I' representation. Standard errors are given in parentheses. Lines that were rejected from the fit are excluded from the statistics. Equilibrium rotational constants, phosphorus spin rotation constants, dipole moment components, and barrier of internal rotation calculated at the ae-CCSD(T)/cc-pwCVQZ level, zero-point vibrational contributions to the rotational constants, centrifugal distortion constants, and barrier of internal rotation calculated at the fc-CCSD(T)/ANO1 level. Ground state rotational constants are estimated as $B_0 = B_e - \Delta B_0$. For further details, see text.

Results and Discussion

C₂H₅CP is an asymmetric top molecule with Ray’s asymmetry parameter of $\kappa = (2B - A - C)/(A - C) = -0.98$. Thus, C₂H₅CP is a highly prolate rotor close to the symmetric limit of -1 . Its two nonzero dipole moments $\mu_a = 1.5$ D and $\mu_b = 0.3$ D (see Table 1) result in a strong *a*-type spectrum and a considerably weaker *b*-type spectrum with the methyl group potentially allowing for internal rotation splitting and energetically low-lying vibrational states giving rise to rather intense vibrational satellite spectra.

Parent Isotopologue

Initial scans of the millimeter-wave regime were performed around a wavelength of 2 mm in search of the characteristic *a*-type line pattern. Indeed, strong transitions were observed soon and were found to be fully compatible with the theoretical predictions on both large and small frequency scales. As can be seen in the top spectrum of Figure 2, the broadband scan around 200 GHz clearly features harmonically related line series, as expected for the *a*-type spectrum of a prolate asymmetric rotor. From coarse visual inspection of this scan alone, the separation between consecutive transitions is about 5 GHz, in very good agreement with the theoretical estimate of $(B + C) = 5.25$ GHz calculated for C₂H₅CP (Table 1). At smaller scales, see the bottom spectrum in Figure 2, the assignment of C₂H₅CP to the carrier of the molecular absorption is secured immediately: As can be seen, the theoretical spectrum can be brought into near-perfect agreement with the dominant transitions of the experimental spectrum when a small shift of only 126 MHz is applied, identifying the experimental lines as belonging to the $J = 33 \leftarrow 32$ transition. The spectroscopic offset of 126 MHz translates into a deviation of merely $126 \text{ MHz}/33 \approx 4 \text{ MHz}$ in $B + C$ between prediction and experiment, corresponding to an effective agreement on the order of one per mill. This small empirical correction permitted immediate detection and assignment of many lines from adjacent rotational transitions over a sizable quantum num-

ber regime.

Comprehensive spectroscopic analysis was finally carried out using the 75–120 GHz, 170–255 GHz, and 340–760 GHz broadband spectra and by tracing line series in Loomis-Wood plots employing the LLWP software.⁴³ Besides the capabilities of LLWP to facilitate spectroscopic assignment and (multicomponent) spectral line profile fitting to evaluate transition frequencies accurately, it has also been designed as a frontend to Pickett’s SPFIT/SPCAT program suite,⁴⁴ hence speeding up the spectroscopic analysis as a whole significantly. Owing to the high quality and predictive power of the CCSD(T) model (Table 1), spectral assignment was a rather straightforward procedure. Furthermore, consistency of line fitting was evaluated and supported using our Python package *Pyckett* which is a Python wrapper around Pickett’s SPFIT and SPCAT program suite adding some very useful functionality². Rather than estimating uniform transition frequency uncertainty, uncertainties of either 20 kHz, 30 kHz, or 40 kHz were assigned via an automated process which is described in greater detail in the Supporting Information.

The final fit comprises 6041 ground state transitions with 4024 unique frequencies spanning quantum number ranges of $4 \leq J \leq 140$ and $0 \leq K_a \leq 25$. The majority of these lines are *a*-type transitions (4340 transitions with 2856 unique frequencies) complemented with *b*-type transitions (1701 transitions with 1223 unique frequencies) that proved more difficult to assign due to their lower intensities. However, LLWP’s Blended Lines Window allowed us to derive accurate line positions even for weak or moderately blended lines. No *A/E*-splitting from internal rotation of the methyl group was observed. The final fit parameters are collected in Table 1. As can be seen, the full set of sextic and five octic centrifugal distortion pa-

²This work made extensive use of Pycketts CLI tools `pyckett_add` and `pyckett_omit` to analyze the influence of adding sensible additional parameters to the Hamiltonian or omitting any of the included parameters from the Hamiltonian. See <https://pypi.org/project/pyckett/> for more information or install with pip via `pip install pyckett`

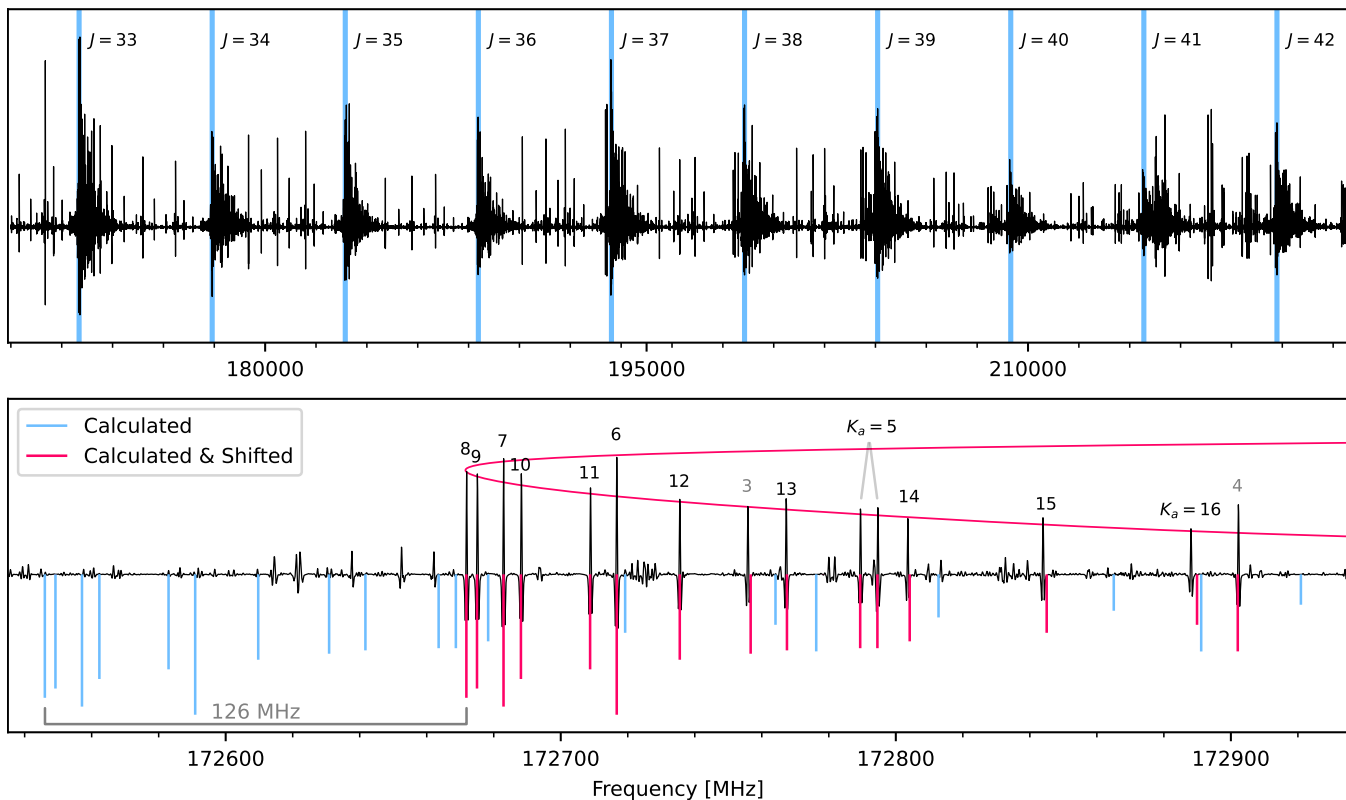


Figure 2: Top: Pure rotational spectrum of $\text{C}_2\text{H}_5\text{CP}$ from 170 to 216 GHz. The typical pattern determined by consecutive a -type rotational transitions is clearly visible. Transitions of the $J_{7,J-7} \leftarrow J-1_{7,J-8}$ series are highlighted in blue and the respective J values are given. The intensities vary due to the frequency-dependence of the source power and pressure in the cell increasing over time. Bottom: One of the first scans taken at 172.7 GHz. The initial theoretical predictions (blue sticks) reproduce the experimental pattern nearly quantitatively when shifted by about +126 MHz, making spectroscopic assignment a straightforward procedure. The red trendline highlights the pattern of the $33_{K_a,33-K_a} \leftarrow 32_{K_a,32-K_a}$ and $33_{K_a,34-K_a} \leftarrow 32_{K_a,33-K_a}$ transitions. For $K_a > 5$ the asymmetry components are overlapping whereas the splitting is still resolved for $K_a = 5$ (indicated by the gray lines). For $K_a = 3$ and $K_a = 4$ the second asymmetry components lie outside the shown region.

rameters were needed to reproduce the transition frequencies within their experimental uncertainties ($rms = 30$ kHz, $wrms = 1.00$). The agreement between the calculated and the experimental molecular parameters is excellent.

Only a very small number of 25 transitions at 14 unique frequencies were omitted from the fit due to $(\nu_{\text{obs}} - \nu_{\text{calc}}) / \Delta\nu_{\text{obs}}$ values greater than 5. Clearly, at values of about $109 \leq J \leq 114$, the ground vibrational state shows signs of a local perturbation, see Figure 3. From a rudimentary Boltzmann-analysis performed through intensity comparison of vibrational satellites and ground state lines, the vibrational wavenumber is estimated as 170 cm^{-1} hinting toward

the energetically lowest state $\nu_{13} = 1$, the first excited in-plane C-C-P bending mode (see Supporting Information). While a quantitative perturbation treatment is beyond the scope of the present paper, a preliminary fit of the vibrational satellite lines compared against the ground state parameters yields rotation-vibration interaction constants in good agreement with values obtained from the anharmonic force field calculations³, substantiating this assignment. Further yet preliminary inspection of

³Calculations yield $\alpha_{\nu_{13}}^A = 146.32$ MHz, $\alpha_{\nu_{13}}^B = -8.28$ MHz, $\alpha_{\nu_{13}}^C = -3.61$ MHz while a preliminary fit yields $\alpha_{\nu_{13}}^A = 180(3)$ MHz, $\alpha_{\nu_{13}}^B = -8.280(7)$ MHz, $\alpha_{\nu_{13}}^C = -3.613(7)$ MHz.

the ν_{13} vibrational satellite pattern with LLWP provides evidence that the state is not just part of a dyad with the ground vibrational state but part of a polyad with other vibrational states. A comprehensive treatment of the vibrational satellite spectrum will be the subject of future analysis.

Additionally, a -type transitions of the vibrational ground state with $K_a = 22$ and $K_a \geq 26$ show systematic deviations for high J values which are most-likely also a result of the interaction with the ν_{13} vibrational state. Thus the analysis of the parent isotopologue was limited to transitions with $K_a < 26$.

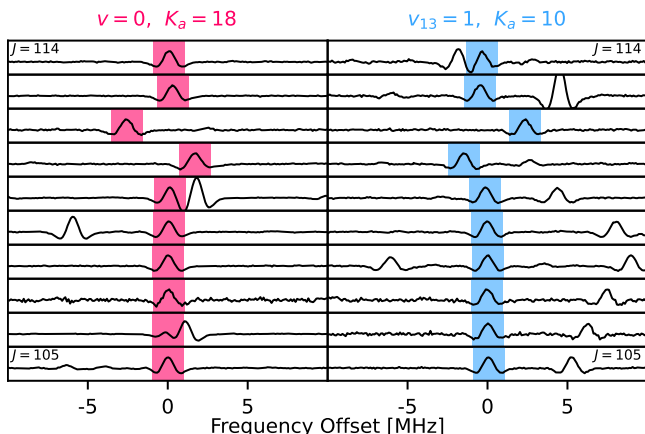


Figure 3: Side-by-side Loomis-Wood plots for the $J_{18,J-17} \leftarrow J-1_{18,J-18}$ series of the vibrational ground state $v = 0$ (left side in red) and the $J_{10,J-9} \leftarrow J-1_{10,J-10}$ series of the energetically lowest vibrationally excited state $\nu_{13} = 1$ (right side in blue). The two sides are almost perfect mirror images with strong deviations for $J = 111$ and $J = 112$. This indicates interactions between the two states centered around the respective $J = 111$ energy levels. The predictions from this work were used as the center frequencies for $v = 0$ while for $\nu_{13} = 1$ a polynomial of degree 2 was fitted to the ten here seen assignments as its preliminary analysis is not sufficiently accurate.

Singly Substituted ^{13}C Isotopologues

While the detection of the singly substituted ^{13}C species proved challenging due to low line

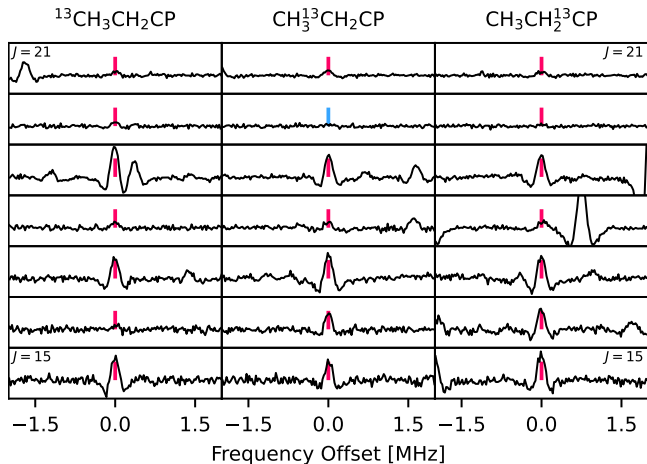


Figure 4: Loomis-Wood plot of the $J_{0,J} \leftarrow J-1_{0,J-1}$ transitions for the three singly substituted ^{13}C species of $\text{C}_2\text{H}_5\text{CP}$. Predictions are shown as sticks in red if the transition is assigned or blue if unassigned. The measured intensity of the lines is highly dependent on the power of the source at the respective frequencies. The overall signal-to-noise ratio is very low for these isotopologues, severely limiting the number of possible assignments.

intensities as well as the overall high line density and line blending (see Figure 4), spectroscopic assignment was finally feasible based on empirically improved predictions obtained by scaling the theoretical rotational parameters of the minor species with correction factors obtained from the parent species (see Supporting Information). This procedure finally enabled the detection of $K_a = 0, 1$ line series very close to the scaled predictions using the LLWP program. Once a valid spectroscopic assignment had been accomplished, assignment of additional series was much easier, however, only a -type spectra up to 500 GHz were assigned with confidence. Many transitions were found blended with close-by strong lines. This was especially severe for $\text{CH}_3\text{CH}_2^{13}\text{CP}$, as its B and C constants are very similar to those of the parent isotopologue. As a result, the quantum number coverage of $\text{CH}_3\text{CH}_2^{13}\text{CP}$ is significantly more limited compared with that of the other two species.

For all rare isotopologues, full quadratic and quartic parameter sets were used. For the sextic parameters only H_J , H_{JK} , H_{KJ} , and h_1 were

Table 2: Molecular parameters of C₂H₅CP and its singly substituted ¹³C isotopologues.

Parameter	CH ₃ CH ₂ CP	¹³ CH ₃ CH ₂ CP	CH ₃ ¹³ CH ₂ CP	CH ₃ CH ₂ ¹³ CP	
<i>A</i>	/ MHz	25 216.122 85(35)	24 834.81(19)	24 696.03(15)	25 115.37(19)
<i>B</i>	/ MHz	2709.143 447(22)	2641.072 28(69)	2686.014 05(83)	2708.970 88(95)
<i>C</i>	/ MHz	2520.638 536(21)	2457.885 62(70)	2495.328 16(71)	2519.453 45(67)
<i>-D_J</i>	/ Hz	-900.7695(38)	-883.46(13)	-861.16(15)	-897.91(23)
<i>-D_{JK}</i>	/ kHz	24.101 222(85)	24.6990(22)	22.2244(20)	24.467(13)
<i>-D_K</i>	/ kHz	-547.7691(34)	-552(19)	-505(20)	-563(18)
<i>d₁</i>	/ Hz	-153.7099(23)	-149.84(20)	-149.67(24)	-155.40(23)
<i>d₂</i>	/ Hz	-8.116 25(97)	-7.635(45)	-8.242(74)	-8.133(43)
<i>H_J</i>	/ mHz	1.504 07(31)	1.507(25)	1.363(25)	1.582(45)
<i>H_{JK}</i>	/ mHz	-14.8371(54)	-17.12(51)	-11.89(45)	-14.1(33)
<i>H_{KJ}</i>	/ Hz	-1.377 47(40)	-1.3748(89)	-1.3072(70)	-1.34(11)
<i>H_K</i>	/ Hz	36.895(11)	a	a	a
<i>h₁</i>	/ μHz	490.70(24)	518(44)	503(53)	549(49)
<i>h₂</i>	/ μHz	69.37(13)	a	a	a
<i>h₃</i>	/ μHz	6.570(15)	a	a	a
<i>L_J</i>	/ nHz	-3.0130(87)	a	a	a
<i>L_{JK}</i>	/ μHz	-2.446(11)	a	a	a
<i>L_{KKJ}</i>	/ μHz	71.50(53)	a	a	a
<i>l₁</i>	/ nHz	-1.3244(74)	a	a	a
<i>l₂</i>	/ pHz	-259.3(50)	a	a	a
Transitions		6016	417	556	163
Lines		4010	282	366	133
<i>RMS</i>	/ kHz	29.7	26.5	25.3	27.7
<i>WRMS</i>		1.00	0.75	0.71	0.77

Note. Fits performed with SPFIT in the S-reduction and the I^r representation. Standard errors are given in parentheses.

^a Parameter was fixed to the parent isotopologue value.

determined which is a result of having only *a*-type transitions assigned. To provide more accurate predictions outside the covered quantum number range, undetermined parameters were set to the main isotopologue values. The resulting molecular parameters are listed in Table 2. The parameters match the scaled predictions very well (see Supporting Information).

While the isotopic data obtained in the present study are by far not sufficient to derive an unconstrained empirical molecular structure of C₂H₅CP they may be used to derive structural information about the carbon backbone. If the experimental ground state rotational constants of all four isotopologues available are first corrected for the effects of zero-point vibration (calculated here at the fc-CCSD(T)/ANO1 level of theory, Table 1 and Supporting Information) prior to structural refinement, then semi-experimental equilibrium structural parameters r_e^{SE} are obtained^{45,46} that may be compared directly to

their *ab initio* values. Using this strategy and keeping the majority of structural parameters fixed at their ae-CCSD(T)/cc-pwCVQZ values, the two C–C bond lengths as well as the C–C–C-angle are determined as $r_{\text{H}_3\text{C}-\text{CH}_2} = 1.5293(2)$ Å, $r_{\text{H}_2\text{C}-\text{CP}} = 1.4647(2)$ Å, and $\alpha_{\text{CCC}} = 112.20(1)^\circ$. These values are in excellent agreement with their ae-CCSD(T)/cc-pwCVQZ counterparts (see Supporting Information). Any extension of the empirical structure determination in the future will require the experimental characterization of a much larger sample of isotopologues, most notably deuterated variants.

Conclusions

Ethyl phosphalkyne, C₂H₅CP, has been detected spectroscopically in the gas phase for the first time. The pure rotational spectrum of the parent isotopic species could be detected, assigned, and analyzed covering frequencies as

high as 760 GHz. In addition, the three singly substituted ^{13}C -species were also observed and characterized up to 500 GHz. The experimental findings agree very well with the results of high-level CCSD(T) calculations.

Future analysis of the vibrational satellite spectrum will be an interesting and challenging task. $\text{C}_2\text{H}_5\text{CP}$ possesses a sizable number of energetically low-lying vibrational modes. Consequently, the vibrational satellite spectrum will comprise contributions not only from fundamental vibrations but also from overtone and combination modes additionally providing ample opportunity for interactions and hence perturbed spectra. As has been shown here, even the ground vibrational state is subject to perturbation at high values of J and K_a .

Now that the pure rotational spectrum of $\text{C}_2\text{H}_5\text{CP}$ in the ground vibrational state has been studied to high accuracy, astronomical searches for this phosphalkyne in suitable sources are feasible. Frequency predictions along with all relevant data (line lists, fit files) will be provided and archived through the Cologne Database for Molecular Spectroscopy, CDMS.^{47,48}

Supporting Information Available

Minimum and transition state structure as well as vibrational wavenumbers and rotation-vibration interaction constants resulting from the quantum-chemical calculations. The calculated and scaled rotational constants for the singly ^{13}C substituted isotopologues. More in detail descriptions of the reproducibility measurements and the automated transition frequency uncertainty assignment procedure.

Acknowledgement LB, SS, and ST gratefully acknowledge the Collaborative Research Center 1601 (SFB 1601 sub-project A4) funded by the Deutsche Forschungsgemeinschaft (DFG, German Research Foundation) – 500700252. MEH acknowledges support by the Bundesministerium für Bildung und Forschung (BMBF) through the Helmholtz research pro-

gram “Materials Systems Engineering” (MSE). JC-G thanks the CNRS national program PCMI (Physics and Chemistry of the Interstellar Medium) and the University of Rennes for a grant.

References

- (1) Snyder, L. E.; Buhl, D. Observations of Radio Emission from Interstellar Hydrogen Cyanide. *Astrophys. J.* **1971**, *163*, L47.
- (2) Zack, L. N.; Halfen, D. T.; Ziurys, L. M. Detection of FeCN ($X^4\Delta_i$) in IRC+10216: A New Interstellar Molecule. *Astrophys. J. Lett.* **2011**, *733*, L36.
- (3) Cernicharo, J.; Marcelino, N.; Pardo, J. R.; Agúndez, M.; Tercero, B.; de Vicente, P.; Cabezas, C.; Bermúdez, C. Interstellar nitrile anions: Detection of C_3N^- and C_5N^- in TMC-1. *Astron. Astrophys.* **2020**, *641*, L9.
- (4) Cernicharo, J.; Cabezas, C.; Pardo, J. R.; Agúndez, M.; Roncero, O.; Tercero, B.; Marcelino, N.; Guélin, M.; Endo, Y.; de Vicente, P. The magnesium paradigm in IRC+10216: Discovery of MgC_4H^+ , MgC_3N^+ , MgC_6H^+ , and MgC_5N^+ . *Astron. Astrophys.* **2023**, *672*, L13.
- (5) McGuire, B. A.; Loomis, R. A.; Burkhardt, A. M.; Lee, K. L. K.; Shingledecker, C. N.; Charnley, S. B.; Cooke, I. R.; Cordiner, M. A.; Herbst, E.; Kalenskii, S. et al. Detection of two interstellar polycyclic aromatic hydrocarbons via spectral matched filtering. *Science* **2021**, *371*, 1265–1269.
- (6) Sita, M. L.; Changala, P. B.; Xue, C.; Burkhardt, A. M.; Shingledecker, C. N.; Lee, K. L. K.; Loomis, R. A.; Momjian, E.; Siebert, M. A.; Gupta, D. et al. Discovery of Interstellar 2-Cyanoindene ($2\text{-C}_9\text{H}_7\text{CN}$) in GOTHAM Observations of TMC-1. *Astrophys. J. Lett.* **2022**, *938*, L12.

- (7) Tyler, J. K. Microwave Spectrum of Methinophosphide, HCP. *J. Chem. Phys.* **1964**, *40*, 1170–1171.
- (8) Burckett-St. Laurent, J. C. T. R.; Cooper, T. A.; Kroto, H. W.; Nixon, J. F.; Ohashi, O.; Ohno, K. The detection of some new phosphalkynes, $\text{RC}\equiv\text{P}$, using microwave spectroscopy. *J. Mol. Struct.* **1982**, *79*, 215–220.
- (9) Bizzocchi, L.; Thorwirth, S.; Müller, H. S. P.; Lewen, F.; Winnewisser, G. Submillimeter-Wave Spectroscopy of Phosphalkynes: HCCCP, NCCP, HCP, and DCP. *J. Mol. Spectrosc.* **2001**, *205*, 110–116.
- (10) Bizzocchi, L.; Degli Esposti, C.; Dore, L.; Puzzarini, C. Lamb-dip millimeter-wave spectroscopy of HCP: Experimental and theoretical determination of ^{31}P nuclear spin-rotation coupling constant and magnetic shielding. *Chem. Phys. Lett.* **2005**, *408*, 13–18.
- (11) Bizzocchi, L.; Degli Esposti, C.; Botschwina, P. Millimeter-wave spectroscopy of HC_3P isotopomers and coupled-cluster calculations: the molecular structure of phosphabutadiyne. *Chem. Phys. Lett.* **2000**, *319*, 411–417.
- (12) Bizzocchi, L.; Degli Esposti, C.; Botschwina, P. Millimeter-wave spectroscopy and coupled cluster calculations for a new phosphorus-carbon chain: HC_5P . *J. Chem. Phys.* **2003**, *119*, 170–175.
- (13) Bizzocchi, L.; Degli Esposti, C.; Botschwina, P. Vibrationally excited states of HC_5P : millimetre-wave spectroscopy and coupled cluster calculations. *Phys. Chem. Chem. Phys.* **2003**, *5*, 4090–4095.
- (14) Bizzocchi, L.; Degli Esposti, C. Pyrolysis of ortho-cyanotoluene and PCl_3 mixtures: the millimeter and submillimeter-wave spectrum of NCCCP. *J. Mol. Spectrosc.* **2003**, *221*, 186–191.
- (15) Bizzocchi, L.; Degli Esposti, C.; Botschwina, P. Vibrationally excited states of NC_4P : millimetre-wave spectroscopy and coupled cluster calculations. *Phys. Chem. Chem. Phys.* **2004**, *6*, 46.
- (16) Ohno, K.; Kroto, H. W.; Nixon, J. F. The Microwave-Spectrum of 1-Phosphabut-3-ene-1-yne, $\text{CH}_2=\text{CHC}\equiv\text{P}$. *J. Mol. Spectrosc.* **1981**, *90*, 507–511.
- (17) Transue, W. J.; Yang, J.; Nava, M.; Sergeev, I. V.; Barnum, T. J.; McCarthy, M. C.; Cummins, C. C. Synthetic and Spectroscopic Investigations Enabled by Modular Synthesis of Molecular Phosphalkyne Precursors. *J. Am. Chem. Soc.* **2018**, *140*, 17985–17991.
- (18) Degli Esposti, C.; Melosso, M.; Bizzocchi, L.; Tamassia, F.; Dore, L. Determination of a semi-experimental equilibrium structure of 1-phosphapropyne from millimeter-wave spectroscopy of CH_3CP and CD_3CP . *J. Mol. Struct.* **2020**, *1203*, 127429.
- (19) Burckett-St. Laurent, J. C. T. R.; Kroto, H. W.; Nixon, J. F.; Ohno, K. The Microwave-Spectrum of 1-Phenylphosphaethyne, $\text{C}_6\text{H}_5\text{C}\equiv\text{P}$. *J. Mol. Spectrosc.* **1982**, *92*, 158–161.
- (20) Samdal, S.; Møllendal, H.; Guillemin, J.-C. Synthesis, Microwave Spectrum, Quantum Chemical Calculations, and Conformational Composition of the Novel Compound Cyclopropylethyldynephosphine ($\text{C}_3\text{H}_5\text{CH}_2\equiv\text{CP}$). *J. Phys. Chem. A* **2014**, *118*, 9994–10001.
- (21) Agúndez, M.; Cernicharo, J.; Guélin, M. Discovery of Phosphaethyne (HCP) in Space: Phosphorus Chemistry in Circumstellar Envelopes. *Astrophys. J.* **2007**, *662*, L91–L94.
- (22) Agúndez, M.; Cernicharo, J.; Guélin, M. New molecules in IRC+10216: confirmation of C_5S and tentative identification of MgCCH , NCCP, and SiH_3CN . *Astron. Astrophys.* **2014**, *570*, A45.

- (23) Endres, C. P.; Martin-Drumel, M.-A.; Zingsheim, O.; Bonah, L.; Pirali, O.; Zhang, T.; Sánchez-Monge, Á.; Möller, T.; Wehres, N.; Schilke, P. et al. SOLEIL and ALMA views on prototypical organic nitriles: C₂H₅CN. *J. Mol. Spectrosc.* **2021**, *375*, 111392.
- (24) Guillemin, J.-C.; Janati, T.; Guenot, P.; Savignac, P.; Denis, J. M. Synthesis of Nonstabilized Phosphaalkynes by Vacuum Gas-Solid HCl Elimination. *Angew. Chem. Int. Ed. Engl.* **1991**, *30*, 196–198.
- (25) Guillemin, J.; Janati, T.; Denis, J. A simple route to kinetically unstabilized phosphaalkynes. *J. Org. Chem.* **2001**, *66*, 7864–7868.
- (26) Raghavachari, K.; Trucks, G. W.; Pople, J. A.; Head-Gordon, M. A fifth-order perturbation comparison of electron correlation theories. *Chem. Phys. Lett.* **1989**, *157*, 479–483.
- (27) Stanton, J. F.; Gauss, J.; Cheng, L.; Harding, M. E.; Matthews, D. A.; Szalay, P. G. CFOUR, Coupled-Cluster techniques for Computational Chemistry, a quantum-chemical program package with contributions from A.A. Auer, R.J. Bartlett, U. Benedikt, C. Berger, D.E. Bernholdt, Y.J. Bomble, O. Christiansen, F. Engel, R. Faber, M. Heckert, O. Heun, M. Hilgenberg, C. Huber, T.-C. Jagau, D. Jonsson, J. Jusélius, T. Kirsch, K. Klein, W.J. Lauderdale, F. Lipparini, T. Metzroth, L.A. Mück, D.P. O’Neill, D.R. Price, E. Prochnow, C. Puzzarini, K. Ruud, F. Schiffmann, W. Schwalbach, C. Simmons, S. Stopkowicz, A. Tajti, J. Vázquez, F. Wang, J.D. Watts and the integral packages MOLECULE (J. Almlöf and P.R. Taylor), PROPS (P.R. Taylor), ABACUS (T. Helgaker, H.J. Aa. Jensen, P. Jørgensen, and J. Olsen), and ECP routines by A. V. Mitin and C. van Wüllen. For the current version, see <http://www.cfour.de>. (visited on 08/15/2019).
- (28) Matthews, D. A.; Cheng, L.; Harding, M. E.; Lipparini, F.; Stopkowicz, S.; Jagau, T.-C.; Szalay, P. G.; Gauss, J.; Stanton, J. F. Coupled-cluster techniques for computational chemistry: The CFOUR program package. *J. Chem. Phys.* **2020**, *152*, 214108.
- (29) Harding, M. E.; Metzroth, T.; Gauss, J.; Auer, A. A. Parallel calculation of CCSD and CCSD(T) analytic first and second derivatives. *J. Chem. Theory Comput.* **2008**, *4*, 64–74.
- (30) Dunning, T. H. Gaussian basis sets for use in correlated molecular calculations. I. The atoms boron through neon and hydrogen. *J. Chem. Phys.* **1989**, *90*, 1007–1023.
- (31) Dunning, T. H.; Peterson, K. A.; Wilson, A. K. Gaussian basis sets for use in correlated molecular calculations. X. The atoms aluminum through argon revisited. *J. Chem. Phys.* **2001**, *114*, 9244–9253.
- (32) Almlöf, J.; Taylor, P. R. General contraction of Gaussian basis sets. I. Atomic natural orbitals for first- and second-row atoms. *J. Chem. Phys.* **1987**, *86*, 4070–4077.
- (33) Peterson, K. A.; Dunning, T. H. Accurate correlation consistent basis sets for molecular core-valence correlation effects: The second row atoms Al-Ar and the first row atoms B-Ne revisited. *J. Chem. Phys.* **2002**, *117*, 10548–10560.
- (34) Watts, J. D.; Gauss, J.; Bartlett, R. J. Open-shell analytical energy gradients for triple excitation many-body, coupled-cluster methods - MBPT(4), CCSD+T(CCSD), CCSD(T), and QCISD(T). *Chem. Phys. Lett.* **1992**, *200*, 1–7.
- (35) Coriani, S.; Marcheson, D.; Gauss, J.; Hättig, C.; Helgaker, T.; Jørgensen, P. The accuracy of ab initio molecular geometries for systems containing second-row atoms. *J. Chem. Phys.* **2005**, *123*, 184107–1–184107–12.

- (36) Gauss, J.; Stanton, J. F. Analytic CCSD(T) second derivatives. *Chem. Phys. Lett.* **1997**, *276*, 70–77.
- (37) Stanton, J. F.; Gauss, J. Analytic second derivatives in high-order many-body perturbation and coupled-cluster theories: computational considerations and applications. *Int. Rev. Phys. Chem.* **2000**, *19*, 61–95.
- (38) Stanton, J. F.; Lopreore, C. L.; Gauss, J. The equilibrium structure and fundamental vibrational frequencies of dioxirane. *J. Chem. Phys.* **1998**, *108*, 7190–7196.
- (39) Gauss, J.; Ruud, K.; Helgaker, T. Perturbation-dependent atomic orbitals for the calculation of spin-rotation constants and rotational g tensors. *J. Chem. Phys.* **1996**, *105*, 2804–2812.
- (40) Puzzarini, C.; Stanton, J. F.; Gauss, J. Quantum-chemical calculation of spectroscopic parameters for rotational spectroscopy. *Int. Rev. Phys. Chem.* **2010**, *29*, 273–367.
- (41) Martin-Drumel, M. A.; van Wijngaarden, J.; Zingsheim, O.; Lewen, F.; Harding, M. E.; Schlemmer, S.; Thorwirth, S. Millimeter- and submillimeter-wave spectroscopy of disulfur dioxide, OSSO. *J. Mol. Spectrosc.* **2015**, *307*, 33 – 39.
- (42) Zingsheim, O.; Bonah, L.; Lewen, F.; Thorwirth, S.; Müller, H. S. P.; Schlemmer, S. Millimeter-millimeter-wave double-modulation double-resonance spectroscopy. *J. Mol. Spectrosc.* **2021**, *381*, 111519.
- (43) Bonah, L.; Zingsheim, O.; Müller, H. S.; Guillemin, J.-C.; Lewen, F.; Schlemmer, S. LLWP – A new Loomis-Wood software at the example of Acetone- $^{13}\text{C}_1$. *J. Mol. Spectrosc.* **2022**, *388*, 111674.
- (44) Pickett, H. M. The fitting and prediction of vibration-rotation spectra with spin interactions. *J. Mol. Spectrosc.* **1991**, *148*, 371–377.
- (45) Vázquez, J.; Stanton, J. F. In *Equilibrium Molecular Structures - From Spectroscopy to Quantum Chemistry*; Demaison, J., Boggs, J. E., Császár, A. G., Eds.; CRC Press, 2011; pp 53–87.
- (46) Kisiel, Z. Least-squares mass-dependence molecular structures for selected weakly bound intermolecular clusters. *J. Mol. Spectrosc.* **2003**, *218*, 58–67.
- (47) Müller, H. S. P.; Thorwirth, S.; Roth, D. A.; Winnewisser, G. The Cologne Database for Molecular Spectroscopy, CDMS. *Astron. Astrophys.* **2001**, *370*, L49–L52.
- (48) Endres, C. P.; Schlemmer, S.; Schilke, P.; Stutzki, J.; Müller, H. S. P. The Cologne Database for Molecular Spectroscopy, CDMS, in the Virtual Atomic and Molecular Data Centre, VAMDC. *J. Mol. Spectrosc.* **2016**, *327*, 95–104.

TOC Graphic

